



**EUROfusion**

WPS1-CPR(17) 17542

J.D. Lore et al.

**Modeling and experimental validation of  
physics enabled by W7-X scraper  
element divertor components**

Preprint of Paper to be submitted for publication in Proceeding of  
27th IEEE Symposium On Fusion Engineering (SOFE)



This work has been carried out within the framework of the EUROfusion Consortium and has received funding from the Euratom research and training programme 2014-2018 under grant agreement No 633053. The views and opinions expressed herein do not necessarily reflect those of the European Commission.

This document is intended for publication in the open literature. It is made available on the clear understanding that it may not be further circulated and extracts or references may not be published prior to publication of the original when applicable, or without the consent of the Publications Officer, EUROfusion Programme Management Unit, Culham Science Centre, Abingdon, Oxon, OX14 3DB, UK or e-mail [Publications.Officer@euro-fusion.org](mailto:Publications.Officer@euro-fusion.org)

Enquiries about Copyright and reproduction should be addressed to the Publications Officer, EUROfusion Programme Management Unit, Culham Science Centre, Abingdon, Oxon, OX14 3DB, UK or e-mail [Publications.Officer@euro-fusion.org](mailto:Publications.Officer@euro-fusion.org)

The contents of this preprint and all other EUROfusion Preprints, Reports and Conference Papers are available to view online free at <http://www.euro-fusionscipub.org>. This site has full search facilities and e-mail alert options. In the JET specific papers the diagrams contained within the PDFs on this site are hyperlinked

# Modeling and Experimental Testing of Heat Fluxes on W7-X Divertor Scraper Elements

J.D. Lore, M. Cianciosa, H. Frerichs, J. Geiger, H. Hoelbe, J. Boscary, and the W7-X team

**Abstract**—Simulations of heat fluxes to the plasma facing components in the Wendelstein 7-X stellarator will be tested in its next operational phase. The simulations consist of core transport calculations that determine the evolution of the kinetic profiles and the toroidal current, which modifies the fluxes to the divertor as the magnetic geometry changes. An additional divertor component, the scraper element, was designed to protect the edges of the primary divertor throughout this evolution during certain high power long pulse operational scenarios. The effect of unknown parameters of the heat flux calculations, namely the cross-field thermal diffusivity and the magnetic field structure, is explored. The predicted scaling of the heat flux widths and magnitudes is presented, along with a new method of calculating the 3D magnetic field structure required to perform the flux calculations.

**Index Terms**—Plasma simulation, Fusion reactors, Plasma transport processes, Wendelstein 7-X

## I. INTRODUCTION

A validated simulation capability to calculate heat and particle fluxes to plasma facing components (PFCs) is a critical need for current and future magnetic confinement fusion devices. First-principles simulations are typically not available or are not tractable to be performed on the timescales of cross-field collisional transport. This is particularly true of stellarators, for which 3D simulations are required due to the general lack of an ignorable symmetry direction as found in tokamaks. Calculation of the fluxes to the PFCs for stellarator operating scenarios therefore often consist of 1.5D core transport simulations (1D radial transport + 2D magnetic surface geometry) to account for the evolution of the kinetic profiles and toroidal current, coupled to a 3D model for the edge transport and PFC geometry. As will be shown, for certain desirable operational scenarios for the Wendelstein 7-X (W7-X) stellarator, these simulations result in a predicted overload of the main divertor PFCs in a region where they have a reduced rating. One proposed solution to this overload scenario is the construction and installation of a set of ten actively-cooled

divertor components known as scraper elements [Peacock 2011]. As the manufacture and installation of these new components adds significant cost, the simulations leading to the prediction of the overload, and the effects of the scraper elements on operation must be validated. In this paper, we present a discussion of these simulations, experiments to assess the effect of scraper elements in the next operational phases of W7-X, and methods for validating the underlying simulations, with a focus on energy transport.

W7-X is a large ( $\langle R \rangle = 5.5$  m,  $\langle a \rangle = 0.53$  m) superconducting stellarator located in Greifswald, Germany. One of the research goals of W7-X is the demonstration of a reactor-relevant divertor design, the island divertor [Grigull 2001]. In the W7-X island divertor the edge rotational transform is chosen to have a rational value, e.g.,  $n/m = 5/5$ , with the 10 divertor modules intersecting the island chain in such a way as to result in ‘stripes’ of heat and particle fluxes to the main divertor PFCs. In a simplified picture, this allows the fluxes to be spread over a large area, and directed to provide good characteristics such as increasing the likelihood of a recycled neutral particle entering a volume to be pumped. The W7-X design is based on a point optimization of the magnetic configuration with respect to several criteria, one of which is a small bootstrap current. Deviation from the current-optimized configurations easily leads to predictions of bootstrap currents on the order of 40 kA, depending on the configuration and plasma scenario [Geiger 2010, Geiger 2015]. This is problematic as a net toroidal current modifies the edge rotational transform, which must be kept fix to have the island chain static relative to the divertor plates. In addition, a finite pressure also results in a modification to the island geometry [Hoelbe 2016]. Without mitigation, these changes to the magnetic geometry modify the PFC fluxes, and can cause overload. In principle, several solutions to this problem are feasible, including radio frequency driven current [Turkin 2006], modification to the existing divertor structure to avoid overload, and development of new configurations. Here we consider only the solution of installing scraper element divertor

*This manuscript has been authored by UT-Battelle, LLC under Contract No. DE-AC05-00OR22725 with the U.S. Department of Energy. The United States Government retains and the publisher, by accepting the article for publication, acknowledges that the United States Government retains a non-exclusive, paid-up, irrevocable, worldwide license to publish or reproduce the published form of this manuscript, or allow others to do so, for United States Government purposes. The Department of Energy will provide public access to these results of federally sponsored research in accordance with the DOE Public Access Plan (<http://energy.gov/downloads/doe-public-access-plan>).*

J.D. Lore is with the Oak Ridge National Laboratory, Oak Ridge TN 37831, USA (e-mail [lorejd@ornl.gov](mailto:lorejd@ornl.gov))

M. Cianciosa is with the Oak Ridge National Laboratory, Oak Ridge TN 37831, USA.

H. Frerichs is with the University of Wisconsin-Madison, Madison WI 53706, USA.

H. Hoelbe and J. Geiger are with the Max Planck Institute for Plasma Physics, Greifswald, Germany.

J. Boscary is with the Max Planck Institute for Plasma Physics, Garching, Germany

components.

The paper is outlined as follows. Section II discusses the schedule and plans for testing the physics basis for the scraper element in the next operational phases of W7-X. Section III presents the simulation of heat fluxes to the divertor components, and how the free parameters will be constrained via experimental measurements. In section IV methods for accounting for the plasma currents external to the equilibrium simulation domain are shown. Finally, discussion and conclusions are given in section V.

## II. EXPERIMENTS TO TEST SCRAPER ELEMENT PHYSICS

The experimental schedule for W7-X is divided into three main phases. OP1.1, already concluded, was the initial demonstration of the device with a limited plasma shape. The next operation phase, OP1.2, will begin in August 2017 with an island divertor installed using non-actively cooled components. This test divertor unit (TDU) has the same shape as the actively cooled divertor. OP1.2 is divided into two phases, OP1.2a and OP1.2b, with two TDU scraper elements installed during a maintenance break. During OP1.2 the energy input during a pulse is limited to 80 MJ. Finally, OP2 will have the full actively cooled divertor installed, with a goal of 30 minute plasmas.

The scenario simulations that result in the predicted overload [Geiger 2010] are not directly accessible in OP1.2 due to limitations on the pulse length. For this reason, a set of magnetic configurations were developed [Hoelbe 2016] to mimic the effect of the OP2 plasma beta and toroidal current using the sweep coils and planar coils, respectively. These configurations will be operated in OP1.2 to validate the simulations that led to the identification of the overload scenario, assess the impact of scraper elements on device operation, and update and refine the predictions for OP2. Of particular interest are verification of the flux patterns and magnitudes that would lead to overload, demonstration of the protection of the edges by the scraper element without predicted overload, and an evaluation of possible deleterious effects of scraper element installation. The latter includes the continued removal of flux from the target edges in the steady-state configuration [Lore 2014], which has the effect of reducing the number of recycled neutral particles entering the pumping volume, degrading the pumping efficiency. A related effect is the new source of recycled neutrals and sputtered carbon impurities due to the additional wetted component. These impacts on steady-state operation must be weighed against the risk of overload without scraper elements, or the probability of success of alternate solutions to the overload problem.

During OP1.2a baseline experiments will be performed to compare the global effects such as particle transport and core impurity influx to OP1.2b experiments where the scraper elements are included. Inter-module comparisons will be possible for local effects, such as the interception of flux in two modules by each scraper element [Hoelbe 2016]. The thermal properties of the TDU scraper element [Titus 2015], given the assumptions used to calculate the scraper element loads [Lore 2014] lead to a design scenario of 6.25s pulses at 2MW of input

power.

## III. CALCULATION OF HEAT FLUXES TO PFCs

W7-X has a large number of diagnostics available to measure quantities related to edge heat transport that will be used to validate predictions of the heat fluxes to the PFCs. These include infrared and visible cameras, Langmuir probes installed on the main divertor and the TDU scraper elements, and thermocouples.

The measurements will be compared to two simulation methods. The first is so-called field line diffusion, where the power crossing the closed flux surfaces is ‘mapped’ to the PFCs by following field lines with ad-hoc cross-field diffusion to move radially from one field line to the next. The method implemented in the DIV3D code [Lore 2014] is used here, which gives similar results as other codes [Bozhenkov 2013]. Field line diffusion was used to design the main W7-X divertor components as well as the scraper element, and is extremely fast as each field line is independent and the calculation can be trivially parallelized. The results are dependent only on the magnetic field geometry, discussed in the following section, and the choice of the (numerical) cross-field diffusivity. In DIV3D this has the form of a ‘magnetic diffusivity’  $D_m = (\Delta_\perp)^2/\Delta_\parallel$ , where the distances  $\Delta_\perp$  and  $\Delta_\parallel$  are step sizes perpendicular and parallel to a field line, respectively. This quantity can be approximately related to plasma physics parameters as  $D_m \sim \chi/T^{1/2}$ , where  $\chi$  is the cross-field thermal diffusivity and  $T$  is a characteristic temperature. Figure 1 shows the strike patterns of 10000 field lines initiated on a closed flux surface onto the W7-X horizontal and vertical divertor components and the scraper element for two values of  $D_m$ , for the predicted OP2 overload scenario, for an input power of 10MW.

By making measurements of the heat flux widths and magnitudes in OP1.2 the field line diffusion model can be validated and the predictions for OP2 refined. In this simple model, the relationship between the magnetic diffusivity and the heat flux magnitude and the width of the wetted area scale as  $D_m^{-1/2}$  and  $D_m^{1/2}$ , respectively, as shown in Fig 2. This scaling does not capture all of the trends of the fluxes to the 3D components, as it can be seen in Fig. 1 that some areas of the divertor are only wetted with sufficiently large cross-field diffusivity. This occurs in regions where the closed surfaces are in close proximity to the PFC.

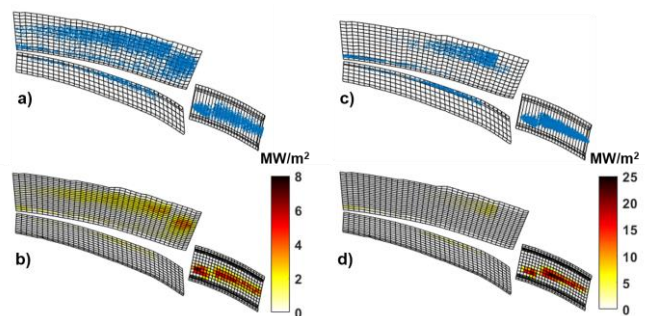


Fig 1. Strike patterns and heat flux magnitudes for two values of the magnetic diffusivity, a-b)  $D_m = 1.2 \times 10^{-5} \text{ m}^2/\text{m}$ , c-d)  $D_m = 1.6 \times 10^{-6} \text{ m}^2/\text{m}$ .

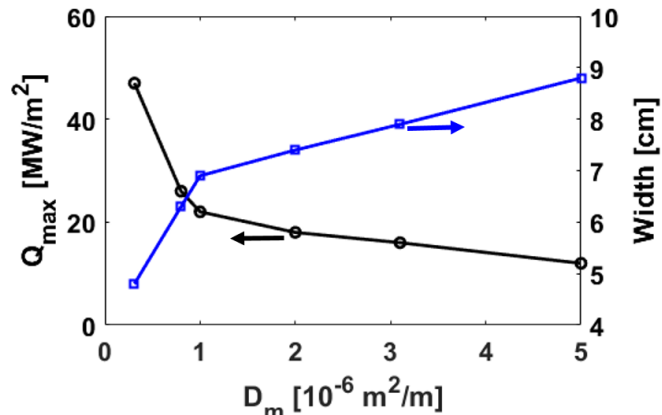


Fig 2. Scaling of peak heat flux and wetted area width (full width half maximum) for a ‘poloidal’ profile on the scraper element as a function of the magnetic diffusivity  $D_m$ .

As this simple model neglects many important physical processes, such as finite parallel temperature gradients and radiation, it is not expected that a fixed magnetic diffusivity can be chosen to reproduce the experimental measurements. For this reason, the comparisons will be used more as a ‘calibration’ of the DIV3D simulations that can be used to rapidly assess operational scenarios.

A much more complete energy transport model is implemented in the 3D edge transport code EMC3-EIRENE [Feng 1997, Feng 1999]. EMC3-EIRENE is a coupling of a 3D fluid plasma transport code (EMC3) which solves the plasma particle continuity, parallel momentum, and energy equations, and a 3D kinetic neutral particle and surface interaction code (EIRENE). Figure 3 shows heat flux patterns calculated by EMC3-EIRENE and DIV3D. The cross-field thermal diffusivity in the EMC3-EIRENE simulation is chosen to be  $3 \text{ m}^2/\text{s}$ , within the range of values used for previous W7-X

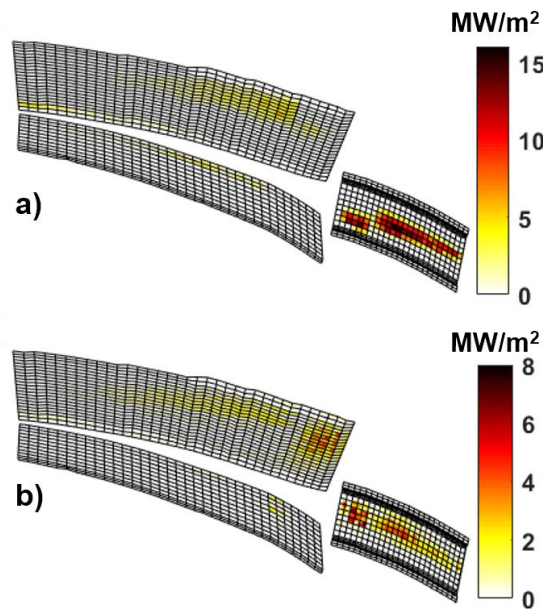


Fig 3. Heat fluxes calculated using a) DIV3D with  $D_m = 3.2 \times 10^{-6} \text{ m}^2/\text{m}$ , and b) EMC3-EIRENE using  $n = 1 \times 10^{19} \text{ m}^{-3}$ ,  $\chi = 3 \text{ m}^2/\text{s}$ .

simulations [Effenberg 2017]. In the DIV3D calculation a value of  $D_m = 3.2 \times 10^{-6} \text{ m}^2/\text{m}$  is used, the same value that was chosen to design the scraper element and match previous W7-X divertor design studies and W7-AS experimental data.

It can be seen that for these choices of input parameters the heat flux magnitude is reduced in EMC3-EIRENE simulation. This is to be expected, as dissipative effects such as radiation and plasma-neutral interactions are included. The EMC3-EIRENE results are more in line with DIV3D calculations with an increased cross-field diffusivity, e.g., Fig. 1b. The flux patterns are similar, with some differences, which could be caused by the dependence of the parallel transport on temperature and density, which is not captured by the field line diffusion model. For this reason, there is not a direct correspondence between the cross-field diffusivity used in EMC3-EIRENE and the magnetic diffusivity used in DIV3D. Scans of the cross-field diffusivity will be used to constrain the EMC3-EIRENE simulations and refine predictions for OP2 scenarios by comparing the results to experimental measurements.

EMC3-EIRENE simulations have the additional advantage of providing particle fluxes to the PFCs and neutral densities in the pumping volumes. These simulation results will be compared to measurements from neutral gas manometers, penning gauges, filterscopes, H-alpha cameras, and various spectroscopic diagnostics. These results are very sensitive to details of the PFC geometry, and the plasma parameters in the edge region, and are not discussed further here.

#### IV. MAGNETIC FIELD MODEL

The heat flux calculations presented in section III require a model for the 3D magnetic field that extends to the PFCs. This is not an issue for a vacuum simulation, where the field is entirely determined by the coil currents, but for finite plasma pressure and current the magnetic field must be calculated using a 3D equilibrium code. The VMEC code [Hirshman 1983] is an equilibrium solver that can calculate the 3D magnetic field assuming nested closed flux surfaces given pressure and toroidal current profiles and either a fixed boundary shape, or a flux enclosed by a calculated last closed magnetic surface shape. VMEC is often used to determine the magnetic geometry of the ‘core’ region of stellarator plasmas due to its rapid solution time, and as many subsequent stellarator transport calculations have been developed to use VMEC output (e.g., determination of neoclassical transport coefficients). However, as the VMEC domain is limited to a closed flux surface the solution cannot extend to the PFCs in stellarators with an island divertor such as W7-X. In principle other codes, such as PIES [Reiman 1986], SPEC [Hudson 2012], SIESTA [Hirshman 2011] or HINT [Harafuji 1989] can be used, but it is of interest to have 3D magnetic field solutions extending to the PFCs that account for the equilibrium currents calculated by VMEC.

There are several methods of ‘extending’ the magnetic field to the PFCs using the VMEC output. A virtual casing principle is one option, in which the 3D equilibrium currents in the VMEC domain are represented by a surface current on the boundary surface. Two methods of applying the virtual casing principle are implemented in the EXTENDER code [Drevlak



2005]. One issue is the degree to which the total field preserves a zero divergence of the magnetic field. A good numerical representation of a divergence free field is necessary not only to accurately follow magnetic field lines, but also to generate an acceptable simulation grid for EMC3-EIRENE, which calculates the conservation of magnetic flux on a field-aligned grid as a related figure of merit. As discussed in Ref [Geiger 2010], the ‘alternate’ virtual casing formulation implemented in EXTENDER results in better flux conservation properties and is thus better suited for use in generating EMC3-EIRENE grids for transport simulations than the ‘traditional’ method (equivalent to the MFBE code [Strumberger 2002]). Here we compare the EXTENDER methods to the result of a new code, BMW (Biot-Savart Magnetic VMEC Vector-Potential). BMW performs a volume integral over the currents in the VMEC domain to calculate the vector potential  $\mathbf{A}$  on a grid spanning the region of interest. This field is added to a Biot-Savart calculation for the vector potential from a current filament representation of the magnetic coil set, and the magnetic field

vector calculated as  $\mathbf{B}=\nabla\times\mathbf{A}$ . This method guarantees divergence free magnetic fields, however a deviation in flux conservation as calculated by EMC3-EIRENE may still exist due to interpolation error and distortion of the numerical mesh.

The three field methods are used to generate Poincare plots for a scenario generating an overload situation at the main divertor edges (22kA toroidal current scenario in [Geiger 2010]), as shown in Fig. 4. The resulting magnetic field can be seen to be similar in terms of the intersection of the edge island chain with the divertor structure, however differences in the core surface shapes exist. In particular, the ‘alternate’ formulation results in a 5/6 island chain near the core, while the BMW calculation has a 5/6 island as well as additional chains near the edge (e.g., 15/17). These islands are observed to decrease in size as the number of poloidal spectral modes used to represent the surface shapes in VMEC is increased.

Each of the three field methods have been used to generate a EMC3-EIRENE grid using the FLARE code [Frerichs 2015]. The flux conservation diagnostic from EMC3-EIRENE reports a maximum deviation of  $\sim 10\%$  for the ‘traditional’ EXTENDER formulation and  $<3\%$  for the alternate formulation, consistent with the results of ref [Geiger 2010]. The BMW formulation resulted in a flux conservation deviation of  $<0.5\%$ . With these results, we have developed and implemented a new method of generating extended magnetic field solutions and EMC3-EIRENE grids using FLARE from VMEC equilibrium solutions.

Energy transport simulations from EMC3-EIRENE are performed using the alternate EXTENDER solution and BMW; the standard (MFBE) grid does not provide adequate flux conservation. A 1D radial profile intersecting the island o-points is shown in Fig. 5. As expected, for the same thermal diffusivity and input power, the presence of core islands reduces the overall energy confinement due to flattening of the temperature profile across the islands. While this is a relatively small effect in this configuration, it may be possible to measure these predicted flat spots in this or other configurations where the island size is increased.

The flux patterns to the PFCs, on the other hand, are largely insensitive to the differences in the magnetic field model, as

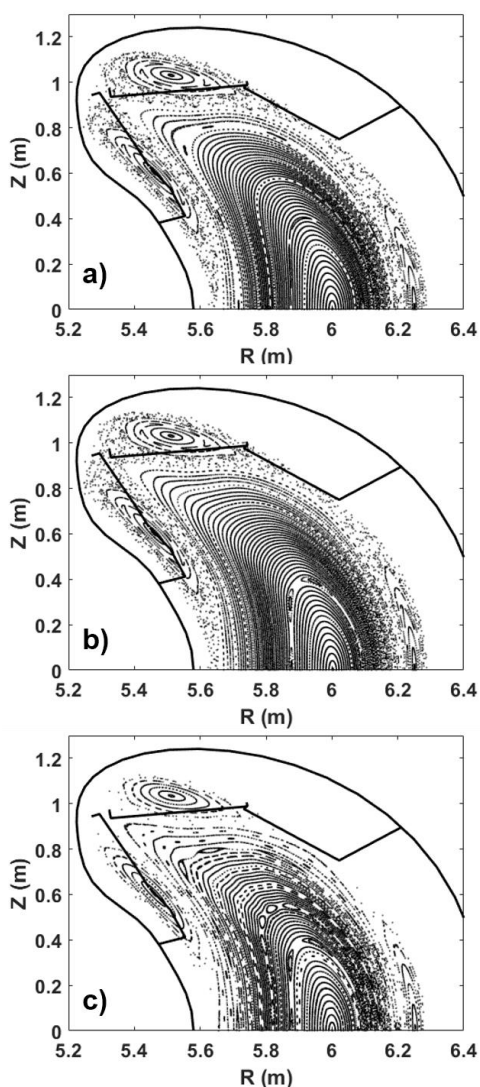


Fig 4. Poincare plots generated using magnetic fields from a) EXTENDER ‘traditional’ (MFBE), b) EXTENDER ‘alternate’, c) BMW.

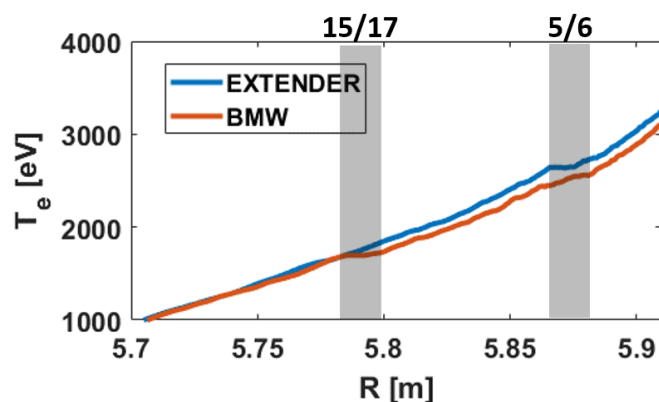


Fig 5. Core electron temperature profiles calculated using EMC3-EIRENE using  $n = 1\times 10^{19} \text{ m}^{-3}$ ,  $\chi = 3 \text{ m}^2/\text{s}$  for the EXTENDER ‘alternate’ and BMW magnetic fields. Island chain  $m/n$  values shown and widths indicated with shaded regions.

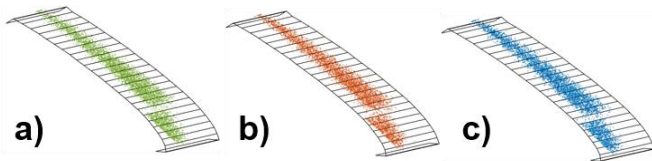


Fig 6. Strike patterns onto the scraper element (pipe shields not plotted) using magnetic field models from a) EXTENDER 'traditional' (MFBE), b) EXTENDER 'alternate', c) BMW.

shown in the flux patterns in Fig. 6 calculated by DIV3D. This is due to the similarity of the intersection of the island geometry with the PFCs, and the finite cross-field diffusion, which largely eliminates differences in the details of the core magnetic structure.

## V. CONCLUSIONS

The physics basis of the scraper elements, and the simulations that led to the identification of the predicted overload scenario, will be tested in the next operational phases of W7-X. The evolution of the magnetic geometry due to pressure and toroidal current in OP2 scenarios will be mimicked using the magnetic coil set. This evolution results in modifications to the fluxes to the PFCs, and measurements of these flux patterns and magnitudes in OP1.2 will provide validation and calibration of the predictions, and allow the OP2 scenarios to be reassessed. Predictions of the heat fluxes and core kinetic profiles are dependent on choices for the cross-field thermal diffusivity as well as the 3D magnetic field structure. The analysis presented here will be used to constrain these parameters using experimental measurements.

## ACKNOWLEDGMENT

This material is based upon work supported by the U.S. Department of Energy, Office of Science, under contract number DE-AC05-00OR22725.

“This work has been carried out within the framework of the EUROfusion Consortium and has received funding from the Euratom research and training programme 2014-2018 under grant agreement No 633053. The views and opinions expressed herein do not necessarily reflect those of the European Commission.”

## REFERENCES

- A. Peacock, J. Kisslinger, J. Boscary, J. Geiger, F. Hurd, R. Koenig, et al., “A proposed scraper element to protect the end of the W7-X divertor target elements,” in Proc. IEEE/NPSS 24th Symp. Fusion Eng., Jun. 2011, pp. 1–5.
- P. Grigull, K. McCormick, J. Baldzuhn, R. Burhenn, R. Brakel, H. Ehmler, et al., “First island divertor experiments on the W7-AS stellarator,” *Plasma Phys. Control. Fusion*, vol. 43, no. 12A, pp. A175–A193, 2001.
- J. Geiger, C. D. Beidler, M. Drevlak, H. Maassberg, C. Nuehrenberg, Y. Suzuki, et al., “Effects of net currents on the magnetic configuration of W7-X,” *Contrib. Plasma Phys.*, vol. 50, no. 8, pp. 770–774, 2010.
- H. Hölbe, T. Sunn Pedersen, J. Geiger, S. Bozhnikov, R. König, Y. Feng, et al., “Access to edge scenarios for testing a scraper element in early operation phases of Wendelstein 7-X,” *Nucl. Fusion*, vol. 56, 026015, 2016.
- Yu. Turkin, H. Maassberg, C. D. Beidler, J. Geiger, and N. B. Marushchenko, “Current Control by ECCD for W7-X,” *Fusion Science and Technology* Vol. 50, Iss. 3, 2006.
- J.D. Lore, T. Andreeva, J. Boscary, S. Bozhnikov, J. Geiger, J.H. Harris, et al., “Design and Analysis of Divertor Scraper Elements for the W7-X Stellarator,” *IEEE TPS* 42, 539 (2014).
- Bozhnikov S.A., Geiger J., Grahl M., Kisslinger J., Werner A. and Wolf R.C. 2013 “Service oriented architecture for scientific analysis at W7-X. An example of a field line tracer” *Fusion Eng. Des.* 88 2997–3006
- Y. Feng, F. Sardei, J. Kisslinger, and P. Grigull, “A 3D Monte Carlo code for plasma transport in island divertors,” *J. Nucl. Mater.*, vols. 241–243, no. 1, pp. 930–934, 1997.
- Y. Feng, F. Sardei, and J. Kisslinger, “3D fluid modeling of the edge plasma by means of a Monte Carlo technique,” *J. Nucl. Mater.*, vols. 266–269, pp. 812–218, Mar. 1999.
- S. P. Hirshman and J. C. Whitson, “Steepest-descent moment method for three-dimensional magnetohydrodynamic equilibria,” *Phys. Fluids*, vol. 26, no. 12, pp. 3553–3568, 1983.
- M. Drevlak, D. Monticello, and A. Reiman, “PIES free boundary stellarator equilibria with improved initial conditions,” *Nucl. Fusion*, vol. 45, no. 7, pp. 731–740, 2005.
- F. Effenberg, Y. Feng, O. Schmitz, H. Frerichs, S.A. Bozhnikov, H. Hölbe, et al “Numerical investigation of plasma edge transport and limiter heat fluxes in Wendelstein 7-X startup plasmas with EMC3-EIRENE” 2017 *Nucl. Fusion* 57 036021
- S.P. Hirshman, R. Sanchez, C.R. Cook, “SIESTA: a scalable iterative equilibrium solver for toroidal applications” *Phys. Plasmas* 18 062504 (2011).
- S. R. Hudson, R. L. Dewar, G. Dennis, M. J. Hole, M. McGann, G. von Nessi, and S. Lazerson, “Computation of multi-region relaxed magnetohydrodynamic equilibria,” *Phys. Plasmas* 19(11), 112502 (2012).
- A. Reiman and H. Greenside, “Calculation of Three-Dimensional MHD Equilibria With Islands and Stochastic Regions”, *Compt. Phys. Commun.* 43, 157-167 (1986).
- Harafuji K et al 1989 *J. Comput. Phys.* 81 169.
- H. Frerichs, O. Schmitz, I. Waters, T. Evans, Y. Feng, V. Soukhanovskii, “Field line reconstruction for edge transport modeling in non-axisymmetric tokamaks configurations”, <http://meetings.aps.org/link/BAPS.2015.DPP.GP12.58> (2015).
- E. Strumberger, S. Günter, P. Merkel, E. Schwarz, C. Tichmann and H.-P. Zehrfeld “Numerical computation of magnetic fields of two- and three-dimensional equilibria with net toroidal current” 2002 *Nucl. Fusion* 42 827.
- Peter H. Titus, H. Zhang, A. Lumsdaine, W. D. McGinnis, J. Lore, et al, “Analysis of the Wendelstein 7-X Test Divertor Unit Scraper Element with Radiation Shields”, *Fusion Science and Technology* Volume 68 2015 Pages 272-276.
- J Geiger, C D Beidler, Y Feng, H Maaßberg, N B Marushchenko and Y Turkin, “Physics in the Magnetic Configuration Space of Wendelstein 7-X”, *Plasma Phys. Control. Fusion* 57 (2015) 014004.